INSTITUTE OF PHYSICS PUBLISHING JOURNAL OF PHYSICS B: ATOMIC, MOLECULAR AND OPTICAL PHYSICS

J. Phys. B: At. Mol. Opt. Phys. **37** (2004) 4539–4550 PII: S0953-4075(04)84805-3

# Projectile electron loss and capture in MeV/u collisions of $U^{28+}$ with $H_2$, $N_2$ and Ar

**R E Olson[1], R L Watson[2], V Horvat[2], A N Perumal[2], Y Peng[2] and Th Stöhlker[3]**

[1] Physics Department, University of Missouri—Rolla, MO 65401, USA
[2] Cyclotron Institute, Texas A&M University, College Station, TX 77843, USA
[3] Atomphysik, GSI-Darmstadt, D-64291 Darmstadt, Germany

Received 10 August 2004, in final form 11 August 2004
Published 8 November 2004
Online at stacks.iop.org/JPhysB/37/4539
doi:10.1088/0953-4075/37/22/012

**Abstract**

Electron capture and loss cross sections for $U^{28+}$ colliding with $H_2$, $N_2$ and Ar were measured at 3.5 and 6.5 MeV/u. These data were used to benchmark *n*-body calculations using the classical trajectory Monte Carlo method. The *n*-body calculations include electrons on both nuclear centres and all electron–electron and electron–nuclear interactions between each centre. For the $U^{28+}$ ion, 36 electrons were incorporated in the calculations ($4s^2 4p^6 4d^{10} 4f^{14} 5s^2 5p^2$), while for the H, N and Ar targets all electrons were used except those for the K-shell of Ar, leading to 39-, 45- and 54-body calculations, respectively. Projectile electron loss was predicted for $U^{28+}$ at energies from 2 to 150 MeV/u. Only for the H-target did the projectile electron loss cross section decrease approximately as $E^{-1}$. The heavier targets exhibited slower energy dependences, contrary to the $E^{-1}$ prediction of one-electron theories. Moreover, the collisional interactions are quite strong with an average of 1.64 and 2.88 electrons removed from the $U^{28+}$ ion at 10 MeV/u in each collision with N and Ar, respectively. These data and calculations were used to assess the vacuum requirements for the SIS-100 synchrotron ring under construction at GSI-Darmstadt. For the residual gases expected to be in the ring, the $U^{28+}$ lifetime was found to be essentially constant as a function of projectile energy, leading to very stringent vacuum requirements.

## 1. Introduction

Heavy ion induced dense plasma experiments planned in both the US and Germany require partially-stripped heavy ions, accelerated to MeV/u energies, and focused onto a target. A low charge state, relative to the equilibrium charge, is necessary to reduce space charge expansion of the beam in the focusing region. However, at MeV/u energies, the projectile is subject to

  

considerable stripping of its electrons. Projectile electron loss results in degraded focusing, and loss of the beam to the walls of the accelerator. In the latter case, these charge-changed fast ions cause sputtering and activation of the surfaces.

In the US, ions under consideration include $K^+$ and $Cs^+$ to $Xe^+$ and possibly $Bi^+$ at energies around 10 to 30 MeV/u (Meier 1998). The German programme has considered low charge state uranium ions such as $U^{7+}$, but now most interest is centred on $U^{28+}$ at energies up to 190 MeV/u. A new enlarged synchrotron ring (SIS-100) will be built at GSI-Darmstadt. For all cases, projectile stripping cross sections are needed in order to assess the vacuum requirements of the accelerators.

Unfortunately, for both the US and European programmes, few to no data exist for the projectile ions at the energies of interest. This is because at these high energies the ion charge states are far below their equilibrium values where experiments can be conveniently performed. Moreover, low charge to mass ratio and high energy are not compatible with existing accelerators. Thus, it is necessary to rely on theoretical calculations for predictions. For the systems of interest, Born calculations by Shevelko *et al* (1998, 2001) and classical trajectory Monte Carlo calculations by Olson (2001) are now available. Also, experimental data exist for partially stripped Ar, Kr and Xe ions in the low MeV/u energy range (Mueller *et al* 2001, Olson *et al* 2002, Watson *et al* 2003 and DuBois *et al* 2003).

The focus of the present work is on the energy dependence of electron capture and loss by $U^{28+}$ ions colliding with $H_2$, $N_2$ and Ar. New experimental measurements have provided total and partial cross sections at energies of 3.5 and 6.5 MeV/u. These data together with cross sections at 1.4 MeV/u, measured several decades ago by Erb (1978) and Franzke (1981) at GSI-Darmstadt, are used to benchmark $n$-body classical trajectory Monte Carlo calculations at the low energy end of a range extending from 2 to 150 MeV/u. It was found that, except for the hydrogen target, multiple electron removal is very important and constitutes approximately 50% of the total projectile electron loss cross section.

## 2. Methods

### *2.1. Theory*

The $n$-body CTMC method has been described in detail previously (Olson *et al* 1989, 1996). The classical Hamiltonian, represented by $6n$ coupled, first-order differential equations are numerically evaluated. The initial electronic states of the projectile ion and target atom are determined from the binding energies of the electrons and their radial expectation values (Carlson *et al* 1970). The time evolution of each collision trajectory involves numerically following the $x$-, $y$- and $z$-positions of each particle along with their conjugate momenta. This is repeated for a series of collisions until adequate statistics are generated on the cross section. In practice about 10 000 to 100 000 trajectories were evaluated for the cross sections given here. Both the electron–electron and electron–nucleus interactions are included between nuclear centres.

Since the collision energies are such that a target centred electron has sufficient energy in the rest frame of the projectile to ionize it, an essential feature of the calculations is the inclusion of both the electron–electron (e–e) and screened nuclear–electron (N–e) interactions between nuclear centres. In the case of stripping from a $U^{28+}$ projectile, this can occur at collision energies above approximately 1.7 MeV/u since the equivalent electron energy at this velocity is approximately equal to the projectile's first ionization potential (930 eV). For lower charge state ions, the e–e interactions become even more important. In general, the (N–e) interaction dominates in hard, small impact parameter collisions, while the (e–e) interaction

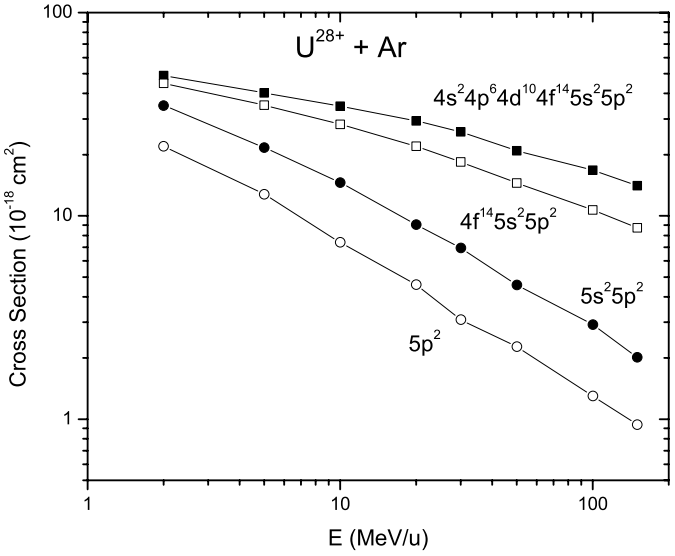


**Figure 1.** $U^{28+}$ + Ar calculated loss cross sections as a function of the size of the basis set on the projectile. Note the change in the energy dependence of the cross sections as the basis set increases.

dominates at large impact parameters. Calculations must encompass the effects of both the e–e and N–e interactions in order to provide reasonable results.

From a theoretical point of view, the complexity of the problem arises mainly from the large number of interactions involved, which increases as $(n^2 - n)/2$ where $n$ is the number of particles. In the *n*CTMC calculations performed here, we have neglected the e–e interactions for electrons on the same centre and have approximated this correlation by using simple static screened interactions between nuclei and each of their electrons (Olson *et al* 1989). It is worth noting, however, that the relevant ionizing interactions (i.e., those between particles on the two centres) are considered in an exact way. Thus, the Hamiltonian for the *n*CTMC method is written as

$$H = (H_o + V_{NP–eP} + V_{NT–eT}) + V_{NP–NT} + V_{NT–eP} + V_{NP–eT} + V_{eP–eT} \quad (1)$$

where $H_o$ is the kinetic energy, and the potential interaction subscripts are denoted by NP (projectile nucleus), NT (target nucleus), eP (projectile electron) and eT (target electron). The terms in parenthesis in equation (1) describe the separate centres that do not produce transitions. It is well known that the internuclear interaction does not contribute significantly to the total cross sections since the nuclei do not exchange a large amount of energy. The simultaneous ionization of both centres is produced by the combined and competing (N–e) and (e–e) interactions.

The *n*-body CTMC calculations are computer intensive. For the $U^{28+}$ ion, it was necessary to utilize 36 outer shell electrons ($4s^24p^64d^{10}4f^{14}5s^25p^2$) in order to obtain convergence on the total cross section. All electrons on the targets were incorporated in the calculations except for Ar where it was deemed unnecessary to include the K-electrons. Thus, counting the nuclei, the number of bodies included in the calculations amounted to 39, 45 and 54 for the H, N and Ar targets, respectively. For the 54-body Ar target calculations, solution of the classical Hamiltonian required following the time evolution of 324 first-order differential equations for each trajectory.

Convergence tests for the stripping of electrons from $U^{28+}$ by Ar are displayed in figure 1. Here, it is shown that the inclusion of the projectile inner shell electrons is

necessary, particularly at the highest collision energies. When only the $U^{28+}$ O-shell outer electrons ($5s^25p^2$) are included, the resulting cross sections are lowered by about 30% at 2 MeV/u. However, at 150 MeV/u this limited basis set underestimates the cross section by approximately a factor of 6.5. Note also that the energy dependence changes appreciably with the inclusion of the inner shells. For the simplest calculation with only the $5p^2$ electrons, the energy dependence is $E^{-0.7}$. In contrast, the full calculation yields a much slower dependence of $E^{-0.3}$. Hence, it is quite apparent that the inner shells make a considerable contribution to the cross section at the higher energies.

It should be noted that the *n*CTMC method explicitly includes the electronic structure of the projectile ion and target atom, and that the energy deposition to the electrons is correctly portrayed. Further, since the CTMC method follows the energy deposition to the heavy particles and uses this information, along with the sequential binding energies to determine the ionization levels, at least to first order, multiple excitation and subsequent Auger ionization are approximated by the calculations. However, the calculation does not account for the radiative stabilization of the ion after excitation. Although expected to be small, the neglect of the radiative decay channel may lead to the calculated cross sections being too large, particularly at high energies where inner shell transitions become important.

### *2.2. Experiment*

An electron cyclotron resonance ion source was used to produce $U^{28+}$ ions which then were injected into the Texas A&M K500 superconducting cyclotron and accelerated to an energy of either 3.5 or 6.5 MeV/u. After travelling through a charge state analysing magnet, the $U^{28+}$ beam passed through a series of four collimators having diameters of 1, 2, 1 and 3 mm, respectively, into a windowless, differentially pumped gas cell having an effective length of 2.08 cm. The beam exited the gas cell through a 3 mm collimator, passed between the poles of a vertical charge dispersing magnet, and stopped in a one-dimensional, position sensitive, microchannel plate detector having a vertical length of 10 cm and a width of 1.5 cm, where the different charge states were identified by their position signals. The target pressure in the gas cell was monitored by a Baratron pressure transducer and the gas flow was regulated with an automatic control valve and flow controller. The $N_2$ and Ar measurements were performed at nominal pressures of 0, 1, 2, 4, 8, 16, 32 and 64 mTorr, while the $H_2$ measurements required higher pressures ranging up to 150 mTorr.

The fraction of ions in each charge state was determined at each pressure by integrating the corresponding peak in the position spectrum. Then, growth curves were constructed by plotting the charge fractions versus the number of target atoms per unit area (i.e., the product of the target atom density and the effective path length). The single collision cross sections were obtained directly from the coefficients of the linear terms of second-order polynomials fitted to the growth curves by the method of least squares. Additional details concerning the experimental methods and analysis procedures are given in Olson *et al* (2002).

## 3. Results

### *3.1. Total cross sections*

The total projectile electron loss and electron capture cross sections for $U^{28+}$ colliding with $H_2$ are presented in figure 2. The experimental data at 1.4 MeV/u are from Franzke (1981), while those at 3.5 and 6.5 MeV/u are from work reported here. The latter cross sections are listed in tables 1 and 2. The Born calculations of Shevelko *et al* (1998) and the *n*CTMC results bracket

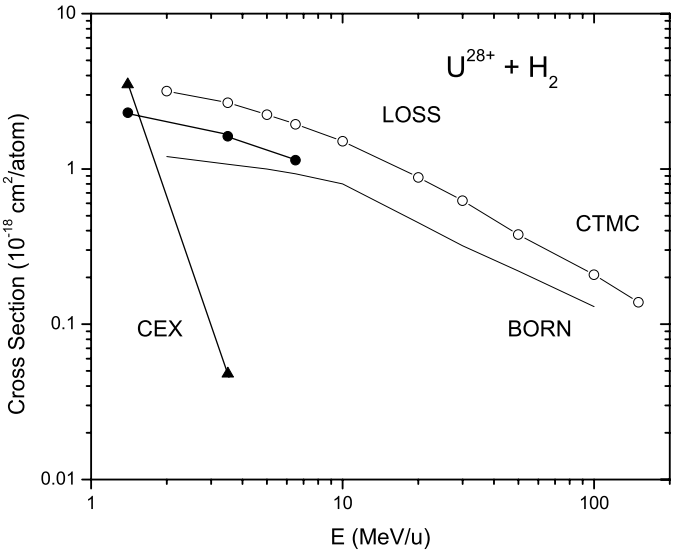


**Figure 2.** $U^{28+}$ electron loss and capture total cross sections for collisions with $H_2$. Note that the cross sections have been divided by two and are given in terms of 'per atom' for the target. The solid symbols at 1.4 MeV/u are data from Franzke (1981). The 3.5 and 6.5 MeV/u data are from this work. The *n*CTMC electron loss cross sections are given by the open circles with attached line. The Born calculations are from Shevelko *et al* (1998, 2001) and denoted by a line. Both the *n*CTMC and Born calculations approach an $E^{-1}$ energy dependence at the highest energies.

**Table 1.** Experimental cross sections for electron capture and loss in collisions of 3.5 MeV/u $U^{28+}$ ions with $H_2$, $N_2$ and Ar ($10^{-18}$ cm$^2$/atom).

| Reaction | $H_2$ | $N_2$ | Ar |
|---|---|---|---|
| 2-capture | $0.071 \pm 0.02$ | $0.20 \pm 0.06$ | |
| 1-capture | $0.048 \pm 0.016$ | $5.03 \pm 0.48$ | $11.20 \pm 0.89$ |
| 1-loss | $1.41 \pm 0.35$ | $9.90 \pm 0.81$ | $15.30 \pm 1.17$ |
| 2-loss | $0.138 \pm 0.042$ | $5.46 \pm 0.51$ | $8.01 \pm 0.68$ |
| 3-loss | $0.0377 \pm 0.013$ | $3.04 \pm 0.34$ | $4.91 \pm 0.47$ |
| 4-loss | $0.0192 \pm 0.0068$ | $1.94 \pm 0.25$ | $3.81 \pm 0.39$ |
| 5-loss | $0.0117 \pm 0.0042$ | $1.06 \pm 0.18$ | $2.97 \pm 0.33$ |
| 6-loss | $0.00839 \pm 0.0030$ | $0.61 \pm 0.13$ | $2.48 \pm 0.30$ |
| 7-loss | $0.26 \pm 0.07$ | $1.93 \pm 0.25$ | |
| 8-loss | $0.12 \pm 0.04$ | $1.68 \pm 0.23$ | |
| 9-loss | $0.093 \pm 0.030$ | $1.25 \pm 0.19$ | |
| 10-loss | | $0.038 \pm 0.013$ | $0.97 \pm 0.17$ |
| 11-loss | | $0.76 \pm 0.14$ | |
| 12-loss | | $0.54 \pm 0.12$ | |
| 13-loss | | $0.34 \pm 0.08$ | |
| 14-loss | | $0.26 \pm 0.07$ | |
| 15-loss | | $0.17 \pm 0.05$ | |
| Total loss | $1.62 \pm 0.35$ | $22.52 \pm 1.07$ | $45.38 \pm 1.62$ |

the experimental projectile electron loss values. The *n*CTMC results are approximately 50% higher than the experimental values. Originally, we speculated that the reason for this is attributable to the fact that the transition probabilities are very small, necessitating a large number of incident trajectories in order to obtain sufficient statistics on the ionization channel.

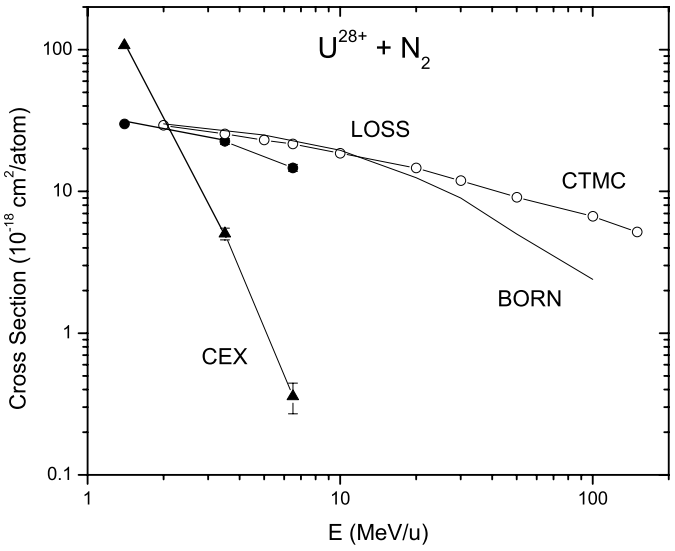


**Figure 3.** $U^{28+}$ electron loss and capture total cross sections for collisions with $N_2$. The notation for the symbols is the same as in figure 1. Between 10 and 100 MeV/u the *n*CTMC cross sections decrease roughly as $E^{-0.45}$.

**Table 2.** Experimental cross sections for electron capture and loss in collisions of 6.5 MeV/u $U^{28+}$ ions with $H_2$, $N_2$ and Ar ($10^{-18}$ cm$^2$/atom).

| Reaction | $H_2$ | $N_2$ | Ar |
|---|---|---|---|
| 1-capture | | $0.33 \pm 0.08$ | $0.39 \pm 0.09$ |
| 1-loss | $1.03 \pm 0.26$ | $7.70 \pm 0.66$ | $10.84 \pm 0.87$ |
| 2-loss | $0.086 \pm 0.028$ | $3.39 \pm 0.36$ | $5.28 \pm 0.49$ |
| 3-loss | $0.017 \pm 0.0061$ | $1.71 \pm 0.23$ | $3.48 \pm 0.37$ |
| 4-loss | $0.0046 \pm 0.0017$ | $0.97 \pm 0.17$ | $2.69 \pm 0.31$ |
| 5-loss | $0.0023 \pm 0.00084$ | $0.53 \pm 0.11$ | $2.52 \pm 0.30$ |
| 6-loss | | $0.22 \pm 0.06$ | $2.02 \pm 0.26$ |
| 7-loss | | $0.10 \pm 0.03$ | $1.68 \pm 0.23$ |
| 8-loss | | $0.043 \pm 0.015$ | $1.15 \pm 0.18$ |
| 9-loss | | $0.033 \pm 0.011$ | $0.99 \pm 0.17$ |
| 10-loss | | | $0.79 \pm 0.15$ |
| 11-loss | | | $0.64 \pm 0.13$ |
| 12-loss | | | $0.47 \pm 0.11$ |
| 13-loss | | | $0.29 \pm 0.08$ |
| 14-loss | | | $0.18 \pm 0.05$ |
| 15-loss | | | $0.13 \pm 0.04$ |
| Total loss | $1.14 \pm 0.26$ | $14.69 \pm 0.82$ | $33.15 \pm 1.25$ |

Round-off errors give rise to a small number of unphysical ionization events, producing a calculated cross section that is too large. However, through grid checks and the testing of integration parameters, we have confirmed that the calculated cross sections are accurate. Above 10 MeV/u, both the Born and the *n*CTMC methods predict similar energy dependences, which is approximately $E^{-0.86}$. This is very close to what one would expect for a collision reaction that is in the perturbation regime where an $E^{-1.0}$ energy dependence is expected.

The results for $N_2$ are shown in figure 3. The notation is the same as for the $H_2$ case. Here, the electron capture channel is primarily dominated by K-shell capture from $N_2$ and it

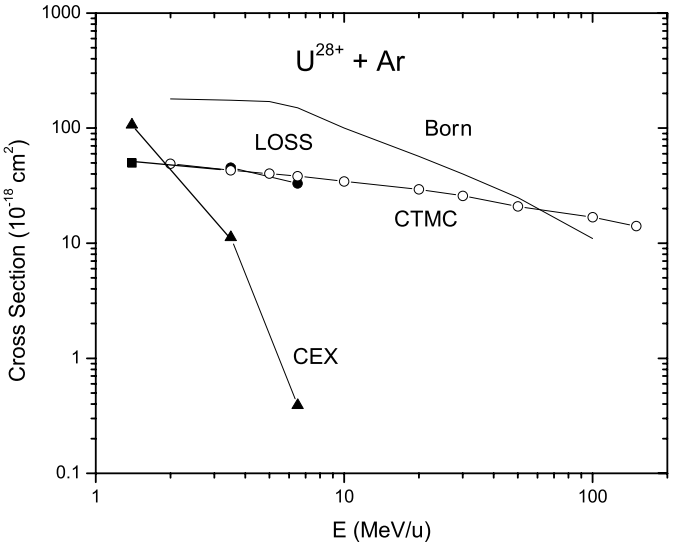


**Figure 4.** $U^{28+}$ electron loss and capture total cross sections for collisions with Ar. The notation for the symbols is the same as in figure 1 except that the 1.4 MeV/u data are from the thesis by Erb (1978). Between 10 and 100 MeV/u the *n*CTMC cross sections decrease approximately as $E^{-0.31}$.

extends to higher energies than in the $H_2$ case. All cross sections and calculations are in good agreement with existing electron loss data. Above 10 MeV/u, the *n*CTMC cross sections are larger than the Born results. The energy dependence of the *n*CTMC cross section decreases as $E^{-0.45}$ between 10 and 100 MeV/u, a much slower slope than for $H_2$, reflecting the increased importance of electron removal from the projectile's inner shells.

The $U^{28+}$ + $N_2$ cross sections are almost identical to those for $Xe^{18+}$ + $N_2$ (Olson *et al* 2002). This was unexpected since the first ionization potential for $Xe^{18+}$ is approximately 570 eV, while that for $U^{28+}$ is 930 eV. From just the ionization energies, one would expect the $U^{28+}$ cross section to be smaller by almost a factor of 2. However, the larger ionization energy of $U^{28+}$ is counteracted by a larger radial expectation value for the outer shell electrons (0.85 $a_0$ for $U^{28+}$ versus 0.78 $a_0$ for $Xe^{18+}$). Also, $U^{28+}$ has more active electrons in its outer shells than $Xe^{18+}$. Note again that the $U^{28+}$ cross section has an energy dependence close to $E^{-0.5}$ which is similar to that of $Xe^{18+}$. This becomes important in the prediction of ion-beam lifetimes in a storage ring.

The results for an Ar target are shown in figure 4. The experimental values at 1.4 MeV/u are from Erb (1978). While the *n*CTMC calculations are in reasonable agreement with the existing measurements, the Born results are approximately a factor of 4 to 5 too large, and have a much different energy dependence above 10 MeV/u. The *n*CTMC cross sections decrease as $E^{-0.31}$, indicating that the heavier the target the slower the projectile electron loss cross section decreases with increasing energy.

The energy dependence is related to the strength of the collision, as may be illustrated by dividing the calculated loss cross sections at 10 MeV/u by the geometric cross section of the outer 5p electrons on the $U^{28+}$ projectile in order to obtain a crude estimate of the probability of electron loss. This ratio is 0.031 for $H_2$, 0.404 for $N_2$ and 0.699 for Ar. Thus, the large discrepancy between the Born and the *n*CTMC results for Ar is probably due to the fact that the *n*CTMC preserves unitarity (i.e., conserves flux), while in the Born approximation the single electron transition probability is multiplied by the number of electrons in each shell and can exceed unit probability for electron removal in many electron systems.

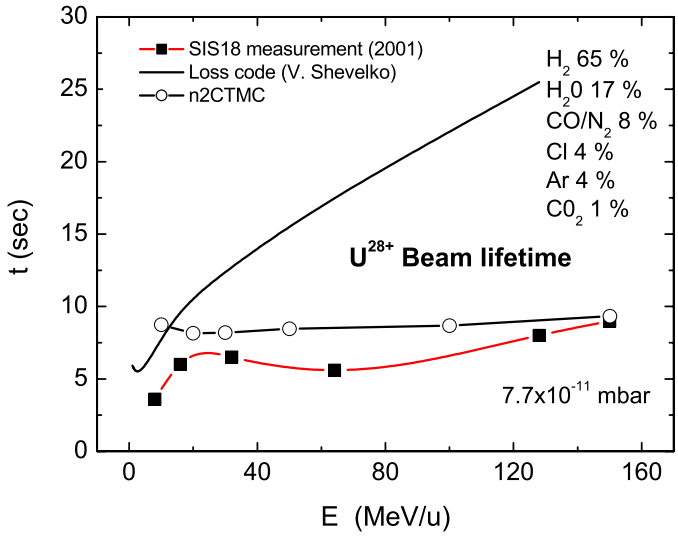


**Figure 5.** Measured $U^{28+}$ beam lifetime as a function of energy at $7.7 \times 10^{-11}$ mbar—solid squares (Krämer *et al* 2002). The line increasing as $E^{+1/2}$ is from the work of Shevelko *et al* (1998, 2001). The open circles that are essentially constant in energy were calculated from the *n*CTMC cross sections presented in figures 2–4.

### *3.2. Ion-beam lifetime*

The theoretical cross sections for energies up to 150 MeV/u may be indirectly tested by employing them to estimate beam lifetimes. The calculated lifetimes may then be compared with measured beam lifetimes from GSI-Darmstadt. In particular, the measured lifetimes display the overall energy dependence of the cross sections. A constant lifetime as a function of energy indicates an average cross section that decreases as $E^{-0.5}$, while a lifetime that increases as $E^{+0.5}$ indicates an average cross section that decreases as $E^{-1.0}$. The calculated $U^{28+}$ loss cross sections presented above were used to estimate the beam lifetime in the present SIS-18 storage ring at GSI-Darmstadt and compared to recent measurements of Krämer *et al* (2002). The measured vacuum constituents are $H_2$ at 65%, $H_2O$ at 17%, $CO/N_2$ at 8%, Cl at 4%, Ar at 4% and $CO_2$ at 1%. The vacuum pressure in the accelerator was $7.7 \times 10^{-11}$ mbar.

The target $Z$-scaling published by Watson *et al* (2003) was used to predict the cross sections for those vacuum constituents not given by the $H_2$, $N_2$ and Ar systems studied above. This scaling leads to an averaged cross section equal to the sum of 1.47 times the cross section of the H target, plus 0.36 times that of N, plus 0.08 times that of Ar. As a representative contribution to the beam lifetime, when the various fractions given above were weighted by their calculated cross sections at 20 MeV/u, the H system contributed 13%, N 63% and Ar 24%. Thus, the mid-$Z$ molecules in the accelerator vacuum dominated the lifetime determination. The heavier constituents, Cl and Ar, also made a major contribution to the lifetime due to their large projectile electron loss cross section while being only a small fraction of the vacuum gases. Although the hydrogen components dominated the vacuum composition, the small cross section for projectile electron loss reduced its contribution.

The calculated and observed beam lifetimes are presented in figure 5. The *n*CTMC results overestimate the measured beam lifetime by about 25%, but display a similar energy dependence. This is in contrast to Born calculations, whose $E^{-1}$ high energy cross

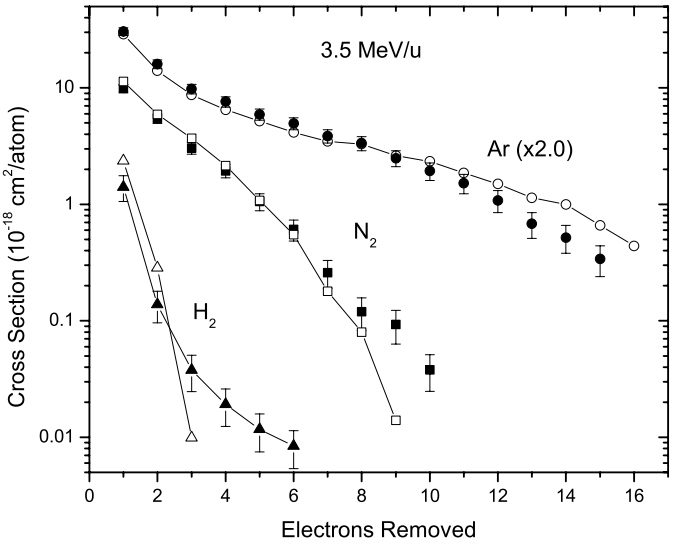


**Figure 6.** Partial loss cross sections for removing $n$-electrons from $U^{28+}$ in 3.5 MeV/u collisions with $H_2$, $N_2$ and Ar. The data are given by the solid points and the $n$CTMC calculations by the open symbols.

section dependence leads to an over optimistic estimate of the lifetime and a lifetime energy dependence that increases as $E^{+0.5}$.

### *3.3. Partial cross sections*

For some applications, it is desirable to know the individual cross sections for multiple electron loss. The removal of more than one electron from the projectile in a single collision may be deleterious to accelerator operation. For example, beam dumps on SIS-100 will be constructed to remove projectiles that undergo single electron loss so that they do not strike the vacuum wall and sputter off unacceptable quantities of ions and atoms (Spiller 2004). Higher stages of projectile ionization will defeat this design.

Comparisons of partial cross sections from theory and experiment (numerical values given in tables 1 and 2) are shown in figures 6 and 7. One can immediately see that the higher $Z$ targets lead to considerably more multiple electron removal than for hydrogen. In fact, for Ar the cross section for the removal of even 15 electrons from $U^{28+}$ is only two orders-of-magnitude smaller than that for single electron removal. In general, the $n$CTMC calculations overestimate the low stages of ionization and underestimate the high stages. This is particularly true for the hydrogen case where the highest stages of ionization are greatly underestimated. In defense of the theory, the last theoretical data points for three times ionized $U^{28+}$ suffer from statistical errors that result from only ten positive events out of the calculation of 50 000 incoming trajectories.

It should be noted that the $n$CTMC method includes not only direct ionization events, but also employs an energy deposition model to describe the high stages of ionization. The electrons are initially given sequential binding energies determined from experiment or sophisticated *ab initio* calculations. After each trajectory, the number of electrons directly ionized from the projectile are recorded. However, the level of excitation of the remaining electrons is also evaluated. This excitation level is then compared to the sequential binding energies of the ion. We assume that inner shell excitations will result in further ionization

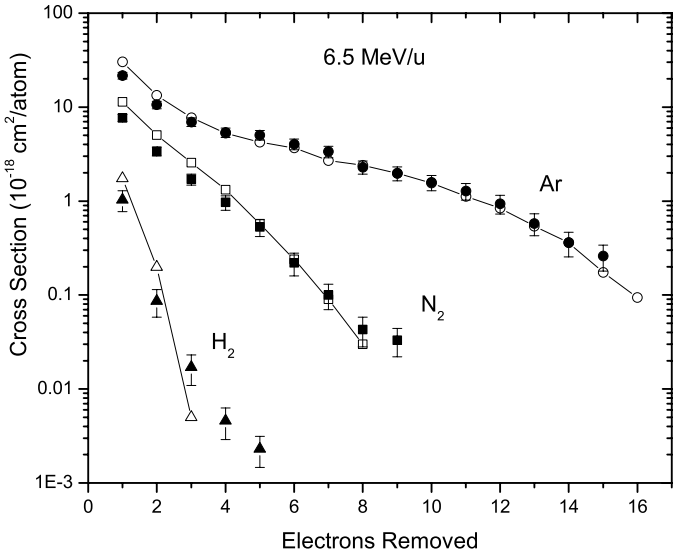


**Figure 7.** Same notation as in figure 8, except the collision energy is 6.5 MeV/u.

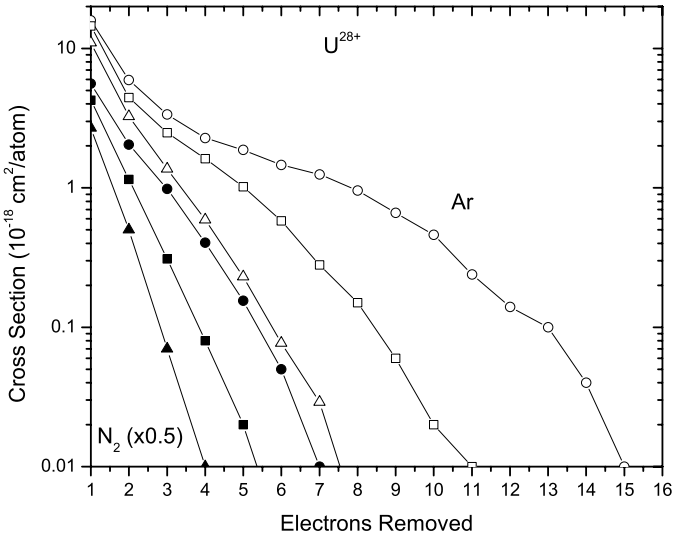


**Figure 8.** Calculated partial loss cross sections for $U^{28+}$ colliding with $N_2$ (solid symbols) and Ar (open symbols). The collision energies presented are 10 MeV/u (circles), 30 MeV/u (squares) and 100 MeV/u (triangles).

due to Auger transitions and this additional level of ionization is recorded. Thus, the energy deposition model inherent in the *n*CTMC method attempts to account for the Auger processes which occur in these collisions. When an inner shell electron is removed, the calculations record the subsequent rearrangement of the electrons as they decay to their ground state.

Calculated cross sections for single and multiple electron loss are displayed in figure 8 for $N_2$ and Ar targets at impact energies of 10, 30 and 100 MeV/u. The $H_2$ case is not shown since the cross sections for multiple electron loss are very small at these energies. The important

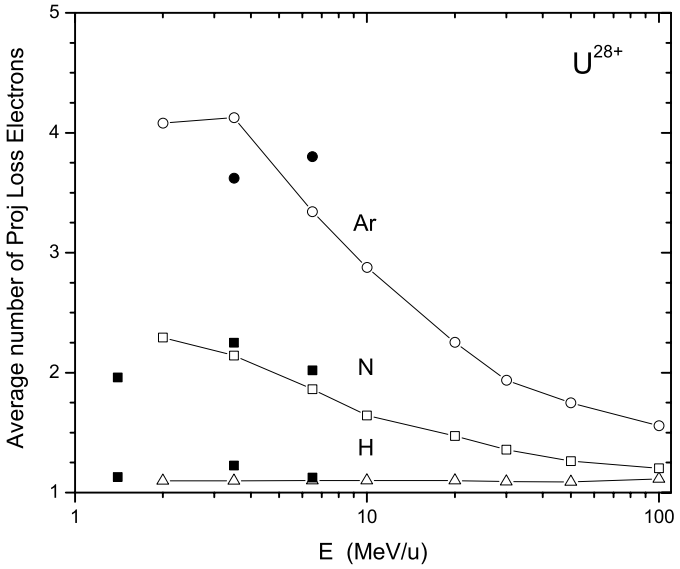


**Figure 9.** The average number of projectile electrons lost per collision calculated using the *n*CTMC method (open symbols). The solid symbols at 3.5 and 6.5 MeV/u are the data from this work. The solid symbols at 1.4 MeV/u are from Franzke (1981). Note that the latter data point for $N_2$ is a lower limit to the number of electrons removed since only cross sections for the loss of one to four electrons were measured.

feature of this comparison is that the extent of multiple electron loss is predicted to decrease rapidly with increasing energy. An explanation for this behaviour can be given in terms of the independent electron model (McGuire and Weaver 1977). At the energies of interest here, the transition probability, $p$, for a single electron transition decreases with increasing energy because the collision time varies as $E^{-0.5}$. Within the independent electron model the probability for removing $n$-electrons is approximately $p^n$. Therefore, when the single electron loss probability decreases, the multiple loss probabilities display a very rapid falloff.

The average number of electrons removed per collision is given by

$$\sum n Q_n \Big/ \sum Q_n,$$

where the summations are over all stages of electron loss with $Q_n$ being the partial cross section for removing $n$-electrons. In figure 9, the *n*CTMC predictions are compared with experiment. The 1.4 MeV/u data point for nitrogen from Franzke (1981) should be considered a lower limit to the true value since only cross sections for the loss of one to four electrons were measured. In general, there is good agreement between theory and experiment. Surprisingly, collisions with the Ar target at energies less than 10 MeV/u result in approximately four electrons being removed from the $U^{28+}$ projectile in each ionizing collision. One also sees the general tendency for multiple electron loss to become less important as the collision energy increases.

## 4. Conclusions

Cross sections for single and multiple electron loss from $U^{28+}$ have been presented for collisions with $H_2$, $N_2$ and Ar. Experimental data at 3.5 and 6.5 MeV/u were used to test predictions

of the *n*CTMC model. Except for the $H_2$ case, where theory overestimates the loss cross section by approximately 50%, there is reasonable agreement with the data. The calculations were then used to predict the loss cross sections for energies up to 150 MeV/u. The resulting beam lifetimes computed from these cross sections were found to be in basic agreement with observations made on the SIS-18 accelerator at GSI-Darmstadt. An important aspect of this comparison is that it confirmed an average loss cross section energy dependence of $E^{-1/2}$ rather than the $E^{-1}$ dependence predicted by one electron models.

Multiple electron loss partial cross sections were also presented. The high-$Z$ Ar target gave rise to considerable multiple electron loss from the $U^{28+}$ projectile, which averaged approximately four electrons per collision for energies less than 10 MeV/u. The *n*CTMC model predicts that the multiple ionization will decrease as the collision energy increases. This latter result has yet to be tested by experiment.

## Acknowledgments

This work supported by Office of Fusion Energy Sciences—Department of Energy and the Robert A Welch Foundation (grant no. A-0355).

## References

Carlson T A, Nestor C W, Wasserman N and McDowell J D 1970 *ORNL-4562*
DuBois R D *et al* 2003 *Phys. Rev.* A **68** 042701
Erb W 1978 *GSI Report P-7-78*
Franzke B 1981 *IEEE, NS-28, 2116*
Krämer A, Boine-Frankenheim O, Mustafin E, Reich-Sprenger H and Spiller P 2002 *Proc. EPAC2002 (Paris)* Online at http://accelconf.web.cern.ch/AccelConf/e02/PAPERS/WEPLE116.pdf
McGuire J H and Weaver L 1977 *Phys. Rev.* A **16** 41
Meier W R 1998 *UCRL-JC-130954*
Mueller D, Grisham L, Kaganovich I, Watson R L, Horvat V, Zaharakis K E and Armel M S 2001 *Phys. Plasmas* **8** 1753
Olson R E 1996 *Atomic, Molecular, and Optical Physics Handbook* ed G W F Drake (College Park, MD: AIP) chapter 56
Olson R E 2001 *Nucl. Instrum. Methods* A **464** 93
Olson R E, Ullrich J and Schmidt-Böcking H 1989 *Phys. Rev.* A **39** 5572
Olson R E, Watson R L, Horvat V and Zaharakis K E 2002 *J. Phys. B: At. Mol. Opt. Phys.* **35** 1893
Shevelko V P, Böhne D and Stöhlker Th 1998 *Nucl. Instrum. Methods* A **415** 609
Shevelko V P, Tolstikhina I Yu and Stöhlker Th 2001 *Nucl. Instrum. Methods* B **184** 295
Spiller P 2004 Private communication
Watson R L, Peng Y, Horvat V, Kim G J and Olson R E 2003 *Phys. Rev.* A **67** 022706